CHEMISTRY
A EUROPEAN JOURNAL

DOI: 10.1002/chem.200701454

Electrochemical Insights into the Mechanisms of Proton Reduction by $[Fe_2(CO)_6\{\mu\text{-}SCH_2N(R)CH_2S\}]$ Complexes Related to the $[2Fe]_H$ Subsite of [FeFe]Hydrogenase

Jean-François Capon, Salah Ezzaher, Frédéric Gloaguen, François Y. Pétillon, Philippe Schollhammer, and Jean Talarmin*[a]

Abstract: Electrochemical investigations on a structural analogue of the $[2Fe]_H$ subsite of $[FeFe]H_2$ases, namely, $[Fe_2(CO)_6\{\mu\text{-}SCH_2N(CH_2CH_2OCH_3)CH_2S\}]$ (**1**), were conducted in $MeCN/NBu_4PF_6$ in the presence of HBF_4/Et_2O or HOTs. Two different catalytic proton reduction processes operate, depending on the strength and the concentration of the acid used. The first process, which takes place around −1.2 V for both HBF_4/Et_2O and HOTs, is limited by the slow release of H_2 from the product of the $\{2H^+/2e\}$ pathway, **1-2H**. The second catalytic process, which occurs at higher acid concentrations, takes place at different potentials depending on the acid present. We propose that this second mechanism is initiated by protonation of **1-2H** when HBF_4/Et_2O is used, whereas the reduction of **1-2H** is the initial step in the presence of the weaker acid HOTs. The potential of the second process, which occurs around −1.4 V (reduction potential of $\mathbf{1\text{-}3H^+}$) or around −1.6 V (the reduction potential of **1-2H**) is thus dependent on the strength of the available proton source.

Keywords: bioinorganic chemistry · electrochemistry · iron · proton reduction · S ligands

Introduction

Since protein crystallography revealed the organometallic nature of the active site of the [FeFe]hydrogenases[1,2] there has been such an explosion of chemical studies devoted to structural, functional, and theoretical modelling of the enzyme H-cluster that the most recent review articles[3] have rapidly become outdated. In the past three years or so, a number of model complexes sharing the $[Fe_2(CO)_{6-n}L_n(\mu\text{-dithiolate})]^z$ framework but featuring different terminal and/or bridging ligands and/or oxidation states have been synthesised, and the aptitude of most of them towards electrocatalytic proton reduction has been tested.[4] Of the diiron dithiolate compounds known to date, two main families emerge based on whether they can be protonated or not. The former category is rapidly growing, since most of the recently synthesised compounds have either electron-donor ligands that make the diiron site sufficiently basic to undergo protonation under appropriate conditions[5–11] or basic ligand(s) in the coordination sphere (terminal ligand[12] or azadithiolate bridge[13–15]).

Whether or not the S–S link of the $[2Fe]_H$ subsite has a N bridgehead atom has not been firmly established to date.[16] However, the prospect of a proton–hydride interaction[17] such as shown in Scheme 1 inspired a number of strategies

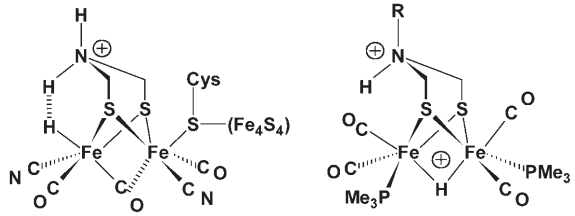

Scheme 1. Possible intermediate[17] involved in reduction of protons and oxidation of H_2 at the active site (H-cluster) of the $[FeFe]H_2$ases (left) and a synthetic diprotonated analogue ($R = CH_2Ph$[24] or $CH_2C_6H_4X$[25]; right).

[a] Dr. J.-F. Capon, S. Ezzaher, Dr. F. Gloaguen, Pr. F. Y. Pétillon, Pr. P. Schollhammer, Dr. J. Talarmin
UMR CNRS 6521 Chimie, Electrochimie Moléculaires et Chimie Analytique
Université de Bretagne Occidentale
6 Av. V. Le Gorgeu, 29285 Brest Cedex (France)
Fax: (+33) 298-017-001
E-mail: jean.talarmin@univ-brest.fr

Supporting information for this article is available on the WWW under http://www.chemeurj.org/ or from the author.

aimed at promoting release or oxidation of H_2 in different types of model compounds.[18–23] This possibility also makes diiron azadithiolate-bridged species attractive models to study in the context of hydrogen production or uptake. Up to now, only two diiron dithiolate complexes that have both a proton and a hydride are known,[24,25] but their structure (Scheme 1), clearly different from that of the H-cluster, prevents direct proton–hydride interaction.

Proton reduction by transition-metal complexes may involve various processes that are initiated by a proton- or electron-transfer step (Scheme 2).[26–28]

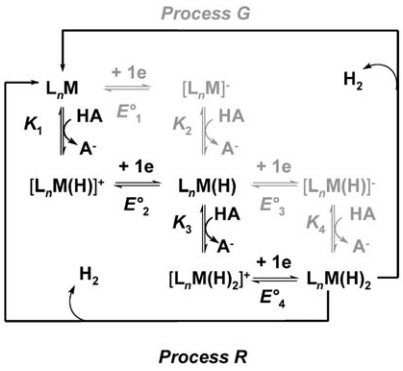

Scheme 2. Mechanisms of proton reduction by transition metals.

Note that Scheme 2 presents an oversimplified picture of the mechanisms involving diiron complexes, since the species shown on the diagonal are not identical in both processes for $[Fe_2(CO)_{6-n}L_n(\mu\text{-dithiolate})]$ compounds. For example, $L_nM(H)$ may either be a μ-H complex (process G) or a species protonated at a bridging or terminal ligand (process R). Moreover, Scheme 2 does not feature structural changes, such as Fe–S bond cleavage, that result from electron transfer[29–32] and generate new sites for protonation, and the possible occurrence of coupled proton- and electron-transfer steps (CPET)[33] is not considered. Nonetheless, it is apparent from Scheme 2 that the pathway that is followed may depend on the strength of the acid used.[12] Switching from the R to the G mechanism can be controlled by the acid strength, either at the initial step of the process [$\log K_1 = pK_a[L_nM(H^+)] - pK_a(HA)$] or at a later stage: $L_nM(H)_2$ can be accessed via a CECE process (R) or via a mixed (CEEC) process if HA is not strong enough to protonate $L_nM(H)$ efficiently.

Diiron hexacarbonyls with a propanedithiolate (pdt, $S(CH_2)_3S$) or a azadithiolate (adt, $SCH_2N(R)CH_2S$) bridge have similar redox potentials,[29,34] but the former do not undergo protonation,[35] while protonation of the latter at the nitrogen atom produces a cation that is reducible at a less negative potential than the parent. This may allow a gain of several hundreds of millivolts ($E^\circ_2 - E^\circ_1$; Scheme 2) in the potential for proton reduction, the mechanisms of which have been thoroughly investigated both experimentally and by theoretical methods in the case of $[Fe_2(CO)_6(\mu\text{-pdt})]$ and $[Fe_2(CO)_6(\mu\text{-edt})]$ (edt = ethanedithiolate, $S(CH_2)_2S$), as well as for diphosphido-bridged hexacarbonyl complexes.[30–32,36,37] In contrast, very little is known about the intimate mechanisms of catalysis by hexacarbonyl azadithiolate-bridged complexes despite the number of reported examples of catalytic proton reduction by these compounds.[14]

We have now examined the electron-transfer chemistry of $[Fe_2(CO)_{6-n}L_n\{\mu\text{-}SCH_2N(R)CH_2S\}]$ complexes both in the absence[29] and in the presence of acid, starting with an hexacarbonyl model that can initially be protonated only at the nitrogen bridgehead atom. Here we report an electrochemical study on $[Fe_2(CO)_6\{\mu\text{-}SCH_2N(CH_2CH_2OMe)CH_2S\}]$ (**1**)[29,38] in the presence of HOTs and HBF_4 with the objective of shedding light on some aspects of the mechanisms by which they catalyse proton reduction.

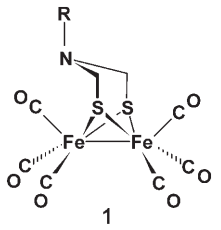

1

R = CH_2CH_2OMe

Results

The electrochemical behaviour of **1** was studied in MeCN/NBu_4PF_6 in the presence of HBF_4/Et_2O and HOTs to assess the impact of the acid strength[39–45] on the overall reduction mechanism. Cyclic voltammetry (CV) of **1** was also briefly studied in the presence of the weaker acid CF_3CO_2H (pK_a = 12.65 in MeCN)[41] for comparison.

Monitoring by cyclic voltammetry of the addition of HBF_4/Et_2O to a solution of $[Fe_2(CO)_6\{\mu\text{-}SCH_2N(CH_2CH_2OMe)CH_2S\}]$ (**1**) in MeCN/NBu_4PF_6 (Figure 1) shows the characteristics of proton reduction catalysed by a protonatable complex (Scheme 2, process R), with an increasing reduction peak at −1.19 V, that is, a potential about 0.4 V less negative than the reduction of the

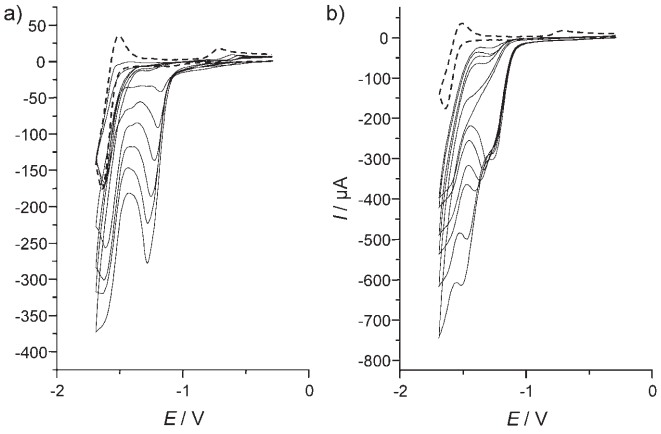

Figure 1. Cyclic voltammetry of **1** (3.6 mM) in MeCN/NBu_4PF_6 in the absence (dashed line), and presence (solid lines) of HBF_4/Et_2O. a) 0.5, 1, 1.55, 2, 2.6, 3.1 equiv acid; b) 3.6, 4.1, 5.1, 6.1, 8.2, 10.2 equiv acid (vitreous carbon electrode, $v = 0.2\ V\,s^{-1}$; potentials are in volts versus Fc^+/Fc).

starting material. The CVs in Figure 1 also evidence that the reduction current around −1.2 V increases markedly only over the addition of the first three or so equivalents of acid, but is scarcely affected when more acid is then added. A new reduction wave ($E_p^{red} \approx -1.4$ V)[46,47] then appears, and its current increases linearly with the amount of acid added (4–10 equiv), consistent with catalytic reduction of protons at this potential. Analogous behaviour was reported for various azadithiolate analogues of **1** in the presence of strong acids,[14a,e,f] and GC analyses of the gaseous contents demonstrated that H_2 is produced during controlled-potential electrolysis under these conditions.[14,15]

The CVs in Figure 2 show that the nature of the acid affects the proton reduction processes, since the potential and

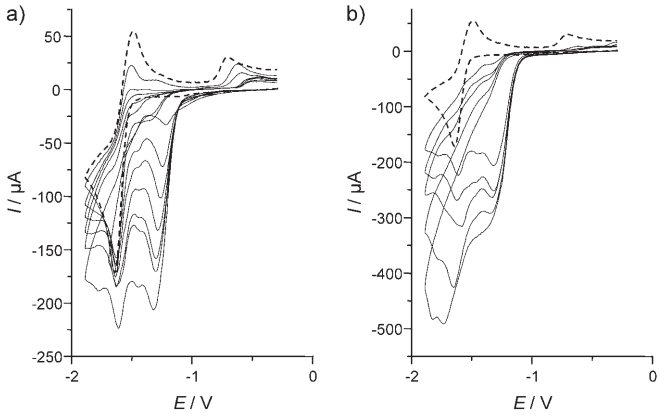

Figure 2. Cyclic voltammetry of **1** (3.6 mM) in MeCN/NBu_4PF_6 in the absence (dashed line) and presence (solid lines) of HOTs. a) 0.5, 1, 1.5, 2, 2.5, 3.1, 4.1 equiv HOTs; b) 4.1, 5.1, 6.1, 8.1, 10.2 equiv HOTs (vitreous carbon electrode, $v = 0.2$ V s^{-1}; potentials are in volts versus Fc^+/Fc).

current of the peak around −1.2 V ($E_p^{red1} = -1.24$ V) are different when HOTs is used in place of HBF_4. Furthermore, the process observed around −1.4 V for HBF_4 when [acid]/[**1**] ≥ 3 is not present for HOTs. An acid-dependent reduction around −1.6 V is observed instead (Figure 2).

As shown in Figure 3, the current of the peak at −1.2 V increases steadily with increasing amount of acid at low acid concentrations, and then levels off when more acid is added. In the initial (linear) part of the curves where pseudo-first-order conditions are not met, the slope of the plot of current versus [acid] is independent of the concentration of the complex and is about 1.3 times larger for HBF_4 than for HOTs. At higher acid concentrations, the current is independent of acid concentration, and for a given concentration of complex, the limiting current at high acid concentration is essentially the same for HBF_4 as for HOTs (Figure 4), which suggests rate-limiting hydrogen elimination under pseudo-first-order conditions.

The occurrence of two reduction processes that depend on both the nature and the amount of added acid prompted us to investigate the different steps of proton reduction cata-

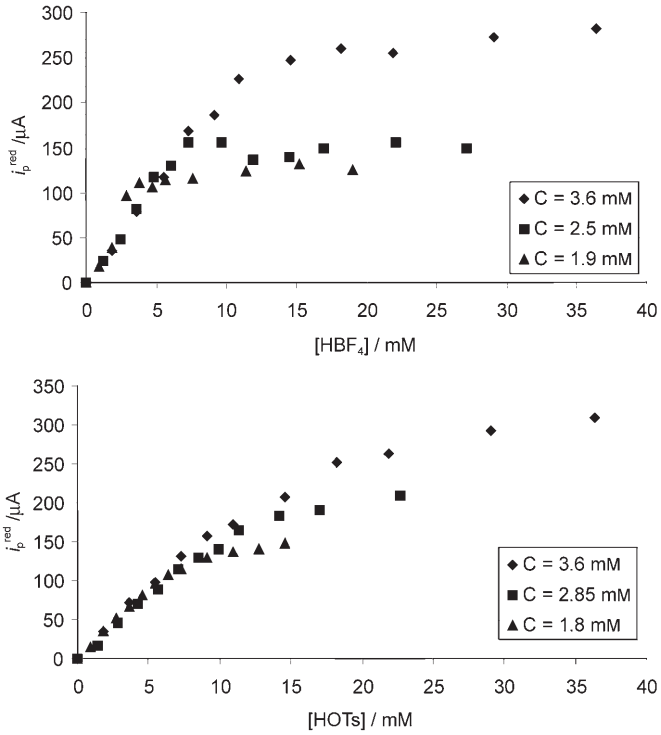

Figure 3. Dependence of the first reduction peak current of **1** upon the concentration of a) HBF_4/Et_2O (top), and b) HOTs (bottom) (MeCN/NBu_4PF_6; the current was measured at about −1.2 V by CV, $v = 0.2$ V s^{-1}, vitreous carbon electrode; the concentration of complex **1** is shown in the diagrams).

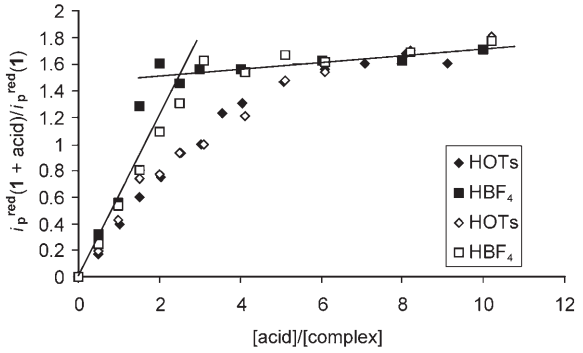

Figure 4. Plots of the normalised reduction peak current [i_p^{red}(**1**+acid)]/i_p^{red}(**1**)] of **1** against the number of added equivalents of acid (HOTs or HBF_4; MeCN/NBu_4PF_6; currents measured at about −1.2 V by CV, $v = 0.2$ V s^{-1}; [**1**]: 3.6 (◇, □), 1.8 (◆), 1.9 mM (■).

lysed by azadithiolate complex **1**, focusing on the less negative process.

The first proton reduction process

Protonation of 1: Treatment of **1** with acid resulted in a shift of 18 cm^{-1} (average) in the ν(CO) bands (Experimental Section), characteristic of ligand-based protonation.[5-b,12,13,14a,b,24,25] Although the protonation site could not be as-

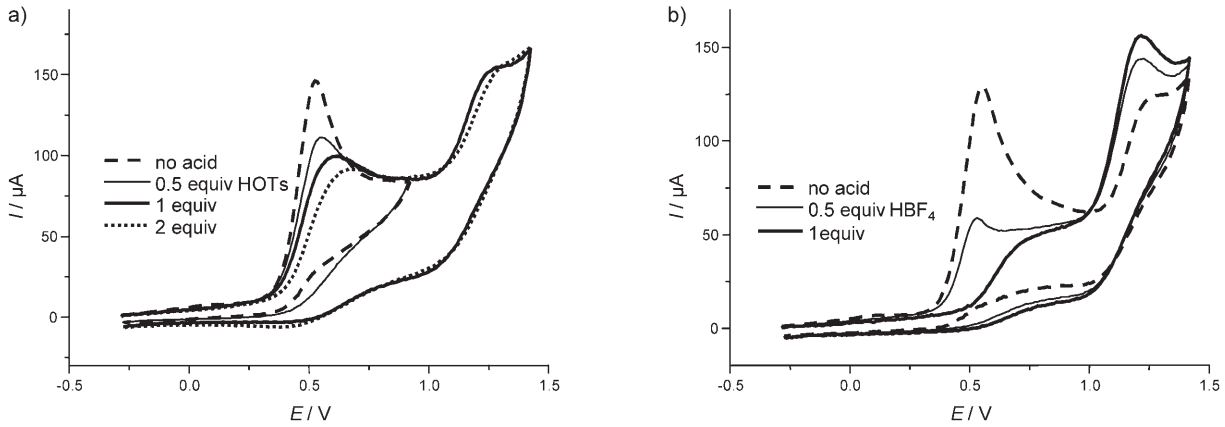

Figure 5. Cyclic voltammetry of the oxidation of **1** in $MeCN/NBu_4PF_6$ in the presence of a) HOTs (2.85 mM **1**) and b) HBF_4/Et_2O (2.5 mM **1**); vitreous carbon electrode, $v = 0.2\ V\,s^{-1}$; potentials are in volts versus Fc^+/Fc.

certained in the present case since **1-H$^+$** could not be isolated, N-protonation has been evidenced in several analogues of **1** in which the R substituent of the N atom allows stabilisation of the NH proton by interaction with a neighbouring heteroatom.[14c,f,25] Furthermore, the X-ray crystal structure of a protonated phosphido-bridged analogue of **1** established that protonation occurred at the nitrogen atom.[48]

The addition of HOTs or HBF_4/Et_2O to a solution of **1** in $MeCN/NBu_4PF_6$ affects the oxidation peak of the complex differently (Figure 5). The peak current is halved upon addition of 0.5 equivalents of HBF_4 to the solution, while the decrease is much less pronounced when 0.5 equivalents or more of HOTs is added. This is consistent with the fact that the acid–base equilibrium in Scheme 3 lies farther to the

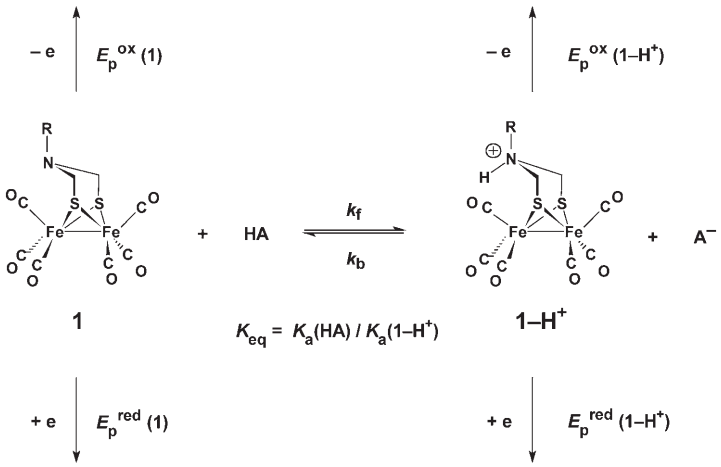

Scheme 3. Acid–base equilibrium involving **1** and **1-H$^+$**.

right when HBF_4/Et_2O is used, because it is a much stronger acid than HOTs in MeCN.[39–45]

During the CV scan, oxidation of **1** at a potential less positive than that of **1-H$^+$** shifts the equilibrium to the left, and this is responsible for the S-shaped oxidation peak of **1** in the presence of acid (Figure 5), typical of a CE process when the current is under kinetic control.[49,50] The addition of 1 equiv of acid to a solution of **1** in $MeCN/NBu_4PF_6$ also produces a new reduction peak assigned to **1-H$^+$** around −1.2 V (Figure 6). The difference between the reduction potentials of **1** and **1-H$^+$** (ca. 0.4 V) is quite similar to that found for other azadithiolate complexes and is consistent with protonation occurring at the nitrogen atom rather than at the Fe–Fe bond; the latter generally results in larger potential shifts.[5,24,51] The peak shape for the reduction of **1-H$^+$** (Figure 6) is not strongly affected by the equilibrium that lies in favour of the protonated complex, particularly when HA is HBF_4. However, the current and the potential of the reduction peak of **1-H$^+$** are dependent on the nature of the acid [for [HA]/[**1**] = 1: $E_p^{red} = -1.19$ V (HBF_4), −1.24 V (HOTs)].

When the weaker acid CF_3CO_2H is used as proton source, no reduction peak is detected around −1.2 V (Figure S2), that is, the amino group is not protonated. This is consistent with the relative pK_a values of the acid (pK_a = 12.65 in MeCN)[41] and of the protonated N bridgehead atom of closely related complexes ($7.6 < pK_a < 10.6$).[13a] The acid-dependent increase in the reduction current around −1.55 V in the presence of CF_3CO_2H suggests that proton reduction under these conditions first requires an electron-transfer step (see process G in Scheme 2). It is therefore likely that, in acetonitrile, $[Fe_2(CO)_6\{\mu\text{-}SCH_2N(R)CH_2S\}]$ complexes cannot be protonated at the N atom by acetic acid (pK_a = 22.3 in MeCN).[41] As a consequence, for $[Fe_2(CO)_6\{\mu\text{-}SCH_2N(R)CH_2S\}]$ complexes in which the R substituent carries a NO_2 group,[52,53] the enhanced current observed in the presence of CH_3CO_2H at a potential substantially less negative than the reduction of the complex most probably arises from a proton-dependent reduction of the nitro group rather than from an initial N-protonation of the complex.[54]

Electrochemical reduction of 1-H$^+$: The CV of **1** in the presence of about one equivalent of HBF_4 recorded at scan rates up to $60\ V\,s^{-1}$ demonstrates that reduction of **1-H$^+$** is a

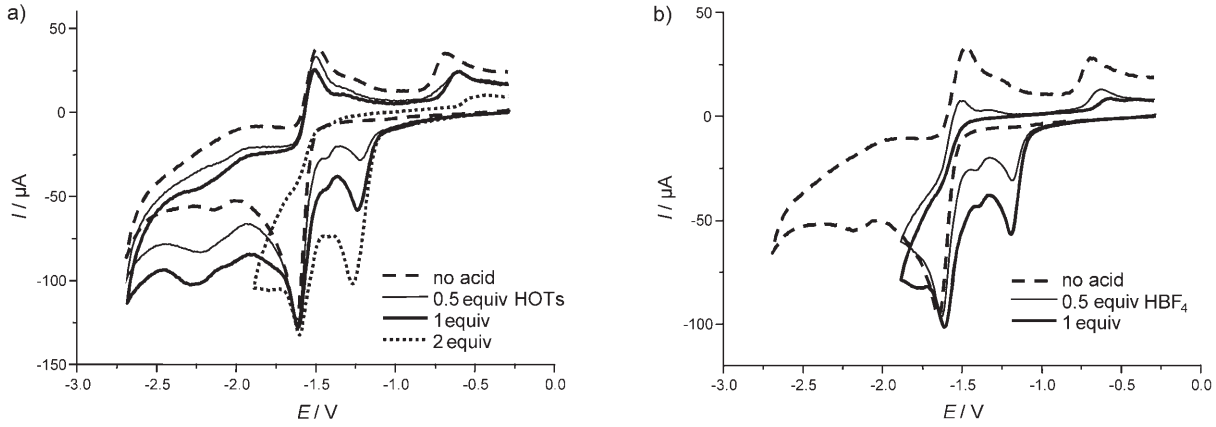

Figure 6. Cyclic voltammetry of the reduction of **1** in $MeCN/NBu_4PF_6$ in the presence of a) HOTs (2.85 mM **1**) and b) HBF_4/Et_2O (2.5 mM **1**); vitreous carbon electrode, $\nu = 0.2\ V\,s^{-1}$; potentials are in volts versus Fc^+/Fc.

chemically irreversible process that regenerates parent complex **1** by a fast follow-up reaction (see Figure S3a in the Supporting Information). The redox features observed at potentials more negative than the reduction of **1-H$^+$** are due to wave splitting[55] of the overall two-electron reduction of **1** that occurs at this scan rate[29] (see Figure S3a in the Supporting Information, broken line). As expected from the CV experiments, controlled-potential reduction of **1** in the presence of 1 equiv of HBF_4/Et_2O regenerated the starting material after the passage of about $1\ F\,mol^{-1}$ **1**. Therefore, the reduction of **1-H$^+$** follows an EC[46,49] mechanism in which the follow-up reaction is either first-order loss of the H atom from **1-H** or a bimolecular reaction between two **1-H** entities that leads to the release of H_2 (Scheme 4).

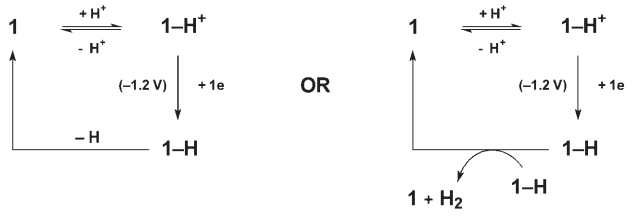

Scheme 4. Loss of H atom from **1-H** and bimolecular reaction between two **1-H** entities with release of H_2

Digital simulations (see Figure S3b in the Supporting Information) of the EC processes in Scheme 4 using DigiElch 3[56] allow one to assign lower limits to the rate constant of the following step of $k \geq 8 \times 10^2\ s^{-1}$ and $k \geq 3 \times 10^6\ M^{-1}\ s^{-1}$, respectively.

Protonation of 1-H and reduction of 1-2H$^+$: Extended Hückel MO calculations[57] show that the LUMO of **1-H$^+$** has substantial Fe–Fe character, like the LUMO of parent complex **1**. Therefore, metal-centred reduction of **1-H$^+$** is likely to increase the pK_a of the diiron site significantly, so that both HOTs and HBF_4 are able to protonate **1-H** at the Fe–Fe bond. This fast reaction produces a cationic complex with a bridging hydride ligand, namely, **1-2H$^+$**, as proposed for various analogues of **1**.[14,24,25] However, our conclusions diverge from those of previously reported studies. Indeed, the current function $i_p/\nu^{1/2}$[46] associated with the reduction at −1.2 V deviates from linearity at slow scan rates after addition of one equivalent of HBF_4/Et_2O to the solution of **1-H$^+$** (i.e., **1**+2 equiv HBF_4, see Figure S4 in the Supporting Information), while $i_p/\nu^{1/2}$ was essentially independent of ν before this addition (i.e., **1**+1 equiv HBF_4). Therefore, the reduction of **1-H$^+$** follows an ECE mechanism in the presence of protons, which signifies that **1-2H$^+$** is reducible at a potential less negative than, or close to, that of **1-H$^+$**, and not at the more negative potential of −1.4 V, as was reported previously for the analogue with $R = CH_2Ph$.[14a,58] Controlled-potential electrolysis ($E_{el} = -1.25$ V, graphite cathode) of a solution of **1** in $MeCN/NBu_4PF_6$ in the presence of two equivalents of HBF_4/Et_2O was complete after consumption of $1.7\ F\,mol^{-1}$ **1**, and the FTIR spectrum of the catholyte was identical to that of a solution made with an authentic sample of **1**. ^1H NMR and FTIR spectra, as well as the CV of the solid isolated from the solution after controlled-potential reduction, confirmed unambiguously that the starting material had been recovered. This is consistent with ECE reduction of **1-H$^+$** at −1.2 V in acidic media. The reduction of $[Fe_2(CO)_6(\mu\text{-}H)(\mu\text{-}pdt)]$ also occurred at a potential less negative than that of $[Fe_2(CO)_6(\mu\text{-}pdt)]$.[30,36]

These results indicate that the conditions for catalytic reduction of protons at −1.2 V are met, since reduction, the current of which increases with increasing concentration of acid, regenerates parent complex **1**. However, this is limited to low acid concentrations when HA is HBF_4. The fact that the maximum current is similar for both acids when $[HA]/[\mathbf{1}] \geq 6$ (Figure 4) suggests that the limiting step is independent of the acid, and may consist of the loss of H_2 from the **1-2H** complex (Scheme 5, process A). For an E_rC' mechanism,[49] the catalytic current is given by Equation (1), where n is the number of electrons involved in the catalytic process, F the Faraday constant, A the electrode area, D the

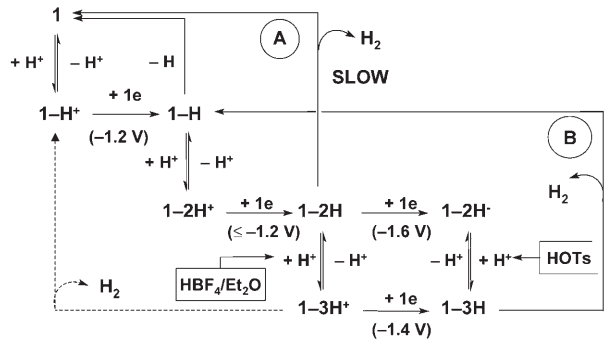

Scheme 5. Catalytic proton reduction processes A and B.

diffusion coefficient of the catalyst, k the rate constant of the catalytic process, and y the order of the reaction with respect to the substrate (HA).[49]

$$I_{cat} = nFA[\mathrm{Cat}](Dk[\mathrm{Substrate}]^{y})^{1/2} \quad (1)$$

At high acid concentrations, the current is independent of [HA] ($y=0$). The rate constant for the release of H_2 from **1-2H** was derived from the slope of the plot of the limiting current at high acid concentrations against the concentration of complex ($k=3.0\pm0.5\ s^{-1}$). The diffusion coefficient of **1** used in the calculations was obtained from CV at fast scan rates ($v>20\ V\,s^{-1}$) in the absence of acid. Under these conditions, the overall two-electron reduction of **1** is resolved into two one-electron steps, the first of which is quasi-reversible.[29]

The reactions in Scheme 5 (process A) are thus proposed to account for the mechanism of the proton reduction path observed at −1.2 V for both HBF_4/Et_2O and HOTs. Figures 1 and 2 show that when the reduction current at this potential ceases to increase, a new acid-dependent process emerges around −1.4 V when HA = HBF_4 (Figure 1) and around −1.6 V when HA = HOTs (Figure 2, [HOTs]/[**1**] > 5).

Switching to the second catalytic process

The fact that the peak around −1.4 V appears only after about four molar equivalents of the strongest acid HBF_4/Et_2O have been added suggests that the difference between the processes when HOTs or HBF_4 is used as a proton source (Figure 7) arises from a protonation step that only the latter is able to achieve efficiently. This is supported by the observation that the peak around −1.4 V diminishes while the reduction current at −1.6 V increases when OTs^- is added to a solution of **1** and an excess of HBF_4 (Figure 8).

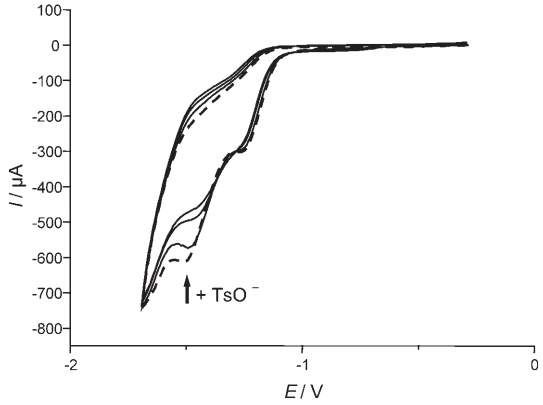

Figure 8. Cyclic voltammetry of **1** (3.6 mM) in the presence of 10 equiv HBF_4/Et_2O before (broken line) and after successive additions of TsO^- ($MeCN/NBu_4PF_6$; vitreous carbon electrode, $v=0.2\ V\,s^{-1}$; potentials are in volts versus Fc^+/Fc)

The second catalytic process thus emerges when the protonation rate of **1-2H** by HBF_4 exceeds the rate of H_2 loss from this complex. The reduction of the resulting **1-3H**$^+$ at −1.4 V generates **1-H** via release of H_2 from **1-3H** (Scheme 5, process B), which is expected to be faster (see Discussion) than H_2 loss from **1-3H**$^+$[59] (dashed arrow in Scheme 5). We tentatively propose that the catalytic reduc-

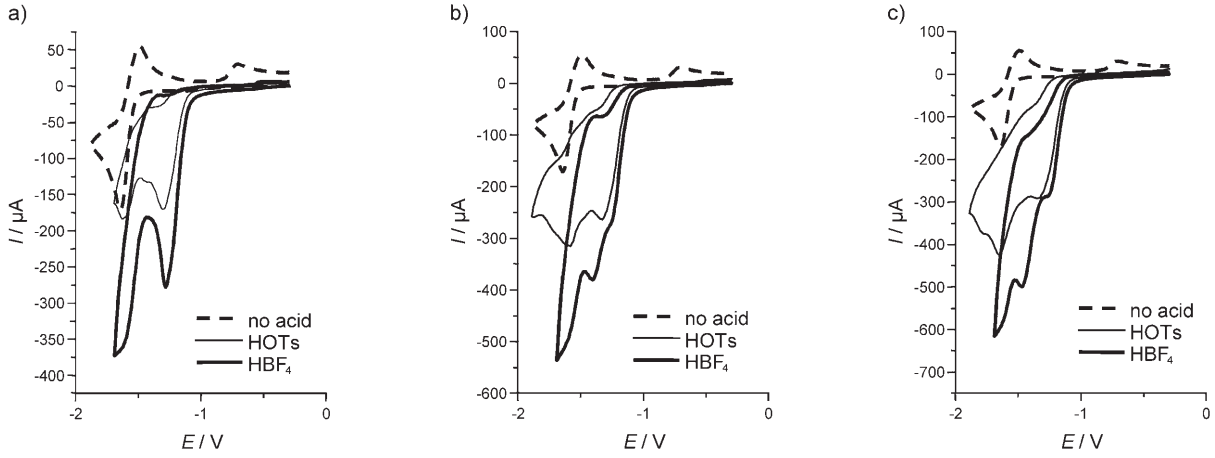

Figure 7. Cyclic voltammetry of **1** (3.6 mM) in $MeCN/NBu_4PF_6$ in the presence of a) 3.1, b) 6.2 and c) 8.2 equiv acid (HOTs or HBF_4; vitreous carbon electrode, $v=0.2\ V\,s^{-1}$; potentials are in volts versus Fc^+/Fc.

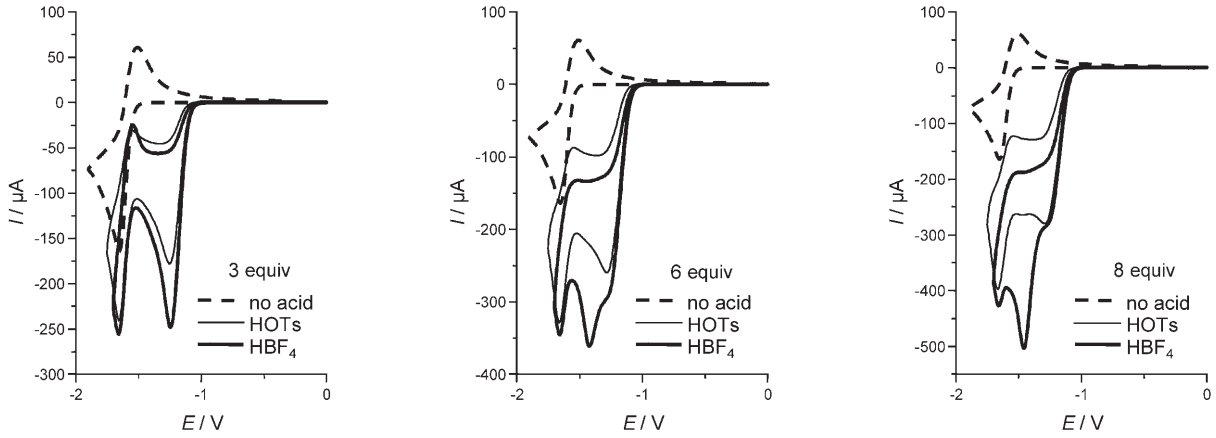

Figure 9. Simulated CV ($v = 0.2\ V\,s^{-1}$) of **1** (3.6 mM) in the presence of different acids ($pK_a = 3$ or 8.3) showing the transition between the catalytic processes A (ca. −1.2 V) and B (ca. −1.4 V or −1.6 V); simulation parameters are given as Supporting Information.

tion at −1.6 V (HA = HOTs) arises from the reduction of **1-2H** followed by protonation of the anion by HOTs to give **1-3H**. Regeneration of **1-H** would thus account for catalytic process B (Scheme 5) at −1.4 V (HA = HBF_4/Et_2O) or −1.6 V (HA = HOTs).

Digital simulations

Digital simulations[56] (see Supporting Information for full details of the procedure) based on the reactions in Scheme 5 were performed to check whether the transition from the process at −1.2 V to that at −1.4 V that is experimentally observed in the presence of HBF_4 could be reproduced by adjusting the equilibrium and rate constants of the protonation steps ($K_{eq} = K_a(HA)/K_a(\mathbf{1}\text{-}n\mathbf{H}^+)$; $n = 1$–3). The CV of **1** was first simulated in the absence of acid, and then in the presence of acids with different pK_a ($pK_a = 3$ and 8.3)[39] with $k = 3\ s^{-1}$ as the rate constant for the release of H_2 from **1-2H** ($k_{exp} = 3.0 \pm 0.5\ s^{-1}$). Owing to the large number of variables, in particular the pK_a values of the different protonated metal complexes used in the simulations are at best rough estimates, the simulations in the presence of acid are only a qualitative test of the validity of the mechanism in Scheme 5. The results of the simulations obtained with the set of constants used are shown in Figure 9 and Figure S6 in the Supporting Information. Comparison with the experimental results (Figure 7 and Figure S6 in the Supporting Information) indicates that the mechanisms proposed in Scheme 5 are consistent with the experimentally observed profiles of the reduction current around −1.2 V as a function of [HA]/[**1**] for HA = HOTs or HBF_4 ([**1**] = 3.6 mM).

Discussion

Comparison of the mechanisms of proton reduction by $[Fe_2(CO)_6(\mu\text{-pdt})]$ and by azadithiolate complex 1: Detailed investigations of the mechanisms of proton reduction by $[Fe_2(CO)_6(\mu\text{-pdt})]$ in THF identified two different catalytic processes at −1.12 V and −1.34 V versus SCE [i.e., −1.62 and −1.84 V versus ferrocene (Fc)].[30] The mechanisms in Scheme 5 display some similarities with those reported for $[Fe_2(CO)_6(\mu\text{-pdt})]$ and also a major difference, that is, initial protonation of the azadithiolate bridge of **1**. As a consequence, process A has no counterpart in the catalytic reduction of protons by $[Fe_2(CO)_6(\mu\text{-pdt})]$, and the energy gain in the catalytic processes supported by the μ-adt complex compared to the μ-pdt analogue (ca. 0.3 V)[60] actually arises from the initial protonation of **1**.

In contrast, process B in which the NH proton is probably not used, exhibits some analogies to process II[30] characterised for the μ-pdt complex. The counterparts of **1-3H$^+$** and **1-3H** in the μ-pdt series regenerate the starting material (process I[30]) and its one-electron reduced product (process II[30]), respectively, upon loss of H_2. The latter is similar to the regeneration of **1-H** from **1-3H** (process B, Scheme 5), which takes place at a potential ca 0.4 V less negative than process II for $[Fe_2(CO)_6(\mu\text{-pdt})]$.[30] However, when HOTs is the proton source for azadithiolate complex **1**, the second catalytic reduction at high acid concentrations occurs around −1.6 V (instead of −1.4 V with HBF_4/Et_2O). Therefore, the difference to the process that occurs at high acid concentration in the case of $[Fe_2(CO)_6(\mu\text{-pdt})]$ is only about 0.2 V when HOTs is used. This arises from the fact that $[HFe_2(CO)_6(\mu\text{-pdt})]^-$ can be protonated by HOTs in THF,[30] while **1-2H** appears not to be protonated by this acid in MeCN. This observation suggests that **1-2H**, that is, $[HFe_2(CO)_6\{\mu\text{-}SCH_2NH(R)CH_2S\}]$, is less basic than $[HFe_2(CO)_6(\mu\text{-pdt})]^-$, although the difference may arise from the different acid–base properties in THF compared to MeCN (the pK_a of HOTs is not known in THF).

Another possible analogy between proton reduction catalysed by $[Fe_2(CO)_6(\mu\text{-pdt})]$ and by complex **1** is the nature of the product preceding release of H_2 in the most negative process. DFT calculations on the products generated by the overall two-electron reduction of **1** identified different isomers of dianion $\mathbf{1}^{2-}$ (Scheme 6), where **B** is more stable than **A** by 31 kJ mol^{-1}.[29]

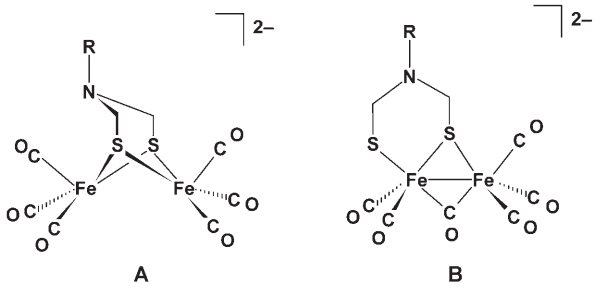

Scheme 6. Isomers of $\mathbf{1}^{2-}$.

Since the diiron core in **1-2H** also accumulated two electrons, one can consider the possibility that **1-2H** and the products derived from it, **1-3H**$^+$ and **1-3H**, also have either the Fe–Fe bond (**A**) or a Fe–S bond cleaved (**B**; Scheme 7, X=NH(R)$^+$).

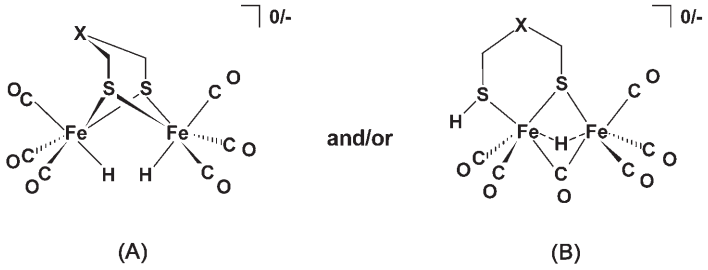

Scheme 7. Possible intermediates involved in proton reduction by complex **1** (X = N(R)H$^+$, **1-3H**$^{+/0}$) and by [$Fe_2(CO)_6$(μ-pdt)] (X = CH_2).

Density functional calculations on the mechanisms of proton reduction by [$Fe_2(CO)_6$(μ-pdt)] identified both isomers in Scheme 7 (X=CH_2) as probable products of the preceding electron- and proton-transfer steps, and showed that release of H_2 was kinetically more favourable from the anion than from the neutral complex,[36] in agreement with the experimental results.[30] It is likely that this also applies to the N-protonated azadithiolate complexes, that is, faster release of H_2 from **1-3H** (Scheme 5, process B) than from **1-3H**$^+$. Two catalytic proton reduction processes were also observed for [$Fe_2(CO)_6$(μ-PhP$(CH_2)_3$PPh)],[32b] that is, a phosphido-bridged analogue of [$Fe_2(CO)_6$(μ-pdt)]. They arise from the release of H_2 by the neutral (slow) and anionic (fast) phosphido counterparts of isomer **A** (Scheme 7). In this case, isomer **B** was not involved, which is consistent with stronger Fe–P than Fe–S bonding, illustrated by the fact that the two-electron reduction of [$Fe_2(CO)_6$(μ-PhP-$(CH_2)_3$PPh)][32b] is chemically more reversible than that of **1**[29] at moderate scan rates.

Release of H_2 from 1-2H: The experimental results and simulated CVs are consistent with limitation of the proton reduction process at −1.2 V by the slow release of H_2 from **1-2H**. This requires either a reaction between two **1-2H** entities, or a rearrangement to allow intramolecular proton–hydride coupling. In the first case, the coupling of the NH proton of one **1-2H** species with the bridging hydride of another would first produce H_2 and two metal species, that is, **1-H**$^+$ and a μ-H complex (**1-μH**$^-$). A second bimolecular reaction would then lead to release of a second H_2 molecule and regenerate the starting material **1**. This may understandably be an overall slow process.

A second possibility is a structural change producing a transient species with a terminally bound hydride ligand that precedes the release of H_2 (Scheme 8). If one assumes that **1-2H** retains the same geometry as **1-2H**$^+$ (however, see above), the rearranged intermediate would resemble the putative intermediate involved in H_2 production and uptake catalysed by the H-cluster[17] (see Scheme 1).

The release of H_2 from **1-2H** should be accelerated in order to favour the lower energy process (A in Scheme 5). From their studies of the thermodynamic properties of Ni and Fe complexes with diphosphine ligands containing internal nitrogen bases, DuBois, Rakowski DuBois et al. elegantly demonstrated that the catalytic efficiency of the complexes towards H_2 production or uptake is greatly improved when the proton relays are positioned so as to ensure an optimal interaction of both the metal and the base with a hydrogen molecule.[23] On the other hand, DFT calculations on diiron models showed that the "rotated" structure in which one of the {$(CO)_3S_2$} pyramids is inverted with respect to the other, which is less stable than the "eclipsed" geometry,[3a,b] could be favoured by introducing electron-donor ligands at one of the Fe centres.[61] Consistent with this, we recently found that the protonation of unsymmetrically disubstituted diiron complexes with a pdt bridge proceeds via initial for-

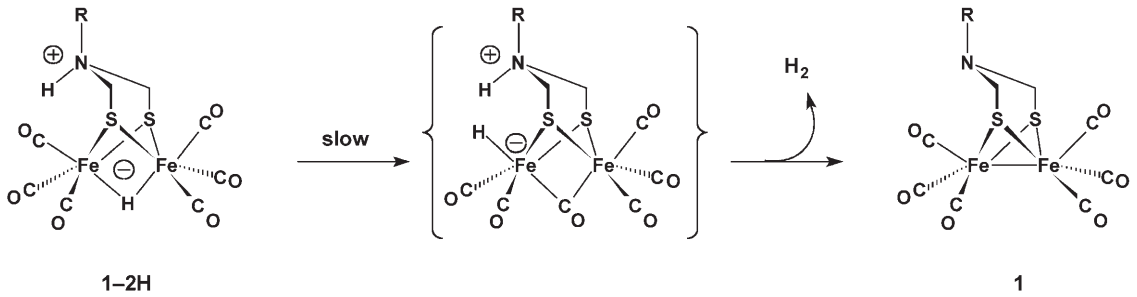

Scheme 8. H_2 release from **1-2H** via a transient species with a terminal hydride ligand.

mation of terminal hydride ligands.[7b,d] The possibility to generate a rotated intermediate upon electrochemical reduction, which would facilitate the release of H_2 from a species such as **1-2H** (Scheme 8), might also be critical at an earlier stage of the process (see below).

Irreversible reduction of 1-H$^+$: The fast chemical step following reduction of **1-H$^+$** regenerates the starting material and thus does not damage the metal catalyst. Although our results demonstrate that it does not prevent protonation of **1-H** either, it may set up a futile loop on the {2H$^+$/2e} path producing H_2 (process A, Scheme 5). A different type of follow-up reaction may occur in the case of a rotated geometry (Scheme 9).

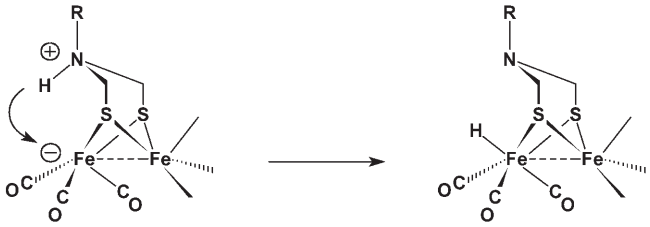

Scheme 9. Hypothetical tautomerisation in a rotated intermediate

Recently, we showed that electrochemical reduction of [$Fe_2(CO)_4$(κ^2-dppe)(μ-dithiolate)] complexes triggers an ETC-catalysed isomerisation to the symmetrical isomer, a process that may involve an anionic intermediate with a rotated geometry.[63] Therefore, the electrochemical reduction of unsymmetrically disubstituted complexes with an azadithiolate bridge in acidic medium might give rise to a proton migration such as that shown in Scheme 9.[64] In contrast to loss of the NH proton, this reaction ensuing the reduction of the N-protonated intermediate (or coupled with it in a CPET process) would lie on the {2H$^+$/2e} path since it produces a terminal hydride and restores a protonation site at the N atom. We have launched a study on proton reduction by [$Fe_2(CO)_4$(κ^2-dppe){μ-$SCH_2N(R)CH_2S$}] complexes to investigate this possibility.

Conclusion

The results of the present work led us to propose two mechanisms for reduction of protons by hexacarbonyl azadithiolate-bridged diiron compounds. Our study confirms that different pathway can be followed, at different stages of the reduction process, depending on the pK_a of the acid employed. The use of acids that are too weak to protonate the nitrogen bridgehead atom (CF_3CO_2H) does not allow the intrinsic properties of azadithiolate complexes to be exploited. In this case, the proton reduction process initiated by an electron-transfer step occurs at a potential very similar to that of the propanedithiolate analogue, because both types of compounds are reduced at comparable potentials. As expected, initial protonation of the nitrogen atom is thus central to lowering the potential of the electrocatalytic proton reduction process. This has no counterpart in the case of the μ-pdt complex.

We also showed that acid strength is again critical at a later stage of the process to drive the reduction towards a lower energy pathway. Interestingly the second catalytic process also occurs at a less negative potential for the azadithiolate complex than for the propanedithiolate analogue. Therefore, the energy gain resulting from initial protonation at the N atom of the bridge is essentially maintained for the second catalytic process, although the NH proton may not be used in this case. For the azadithiolate complexes, both the initial step and the switch between the two catalytic processes are protonation equilibria, while they are both electron-transfer steps in the case of the propanedithiolate analogue.

We proposed that the less negative proton reduction process catalysed by the azadithiolate complexes is limited by slow loss of H_2 from the product formed along the {2H$^+$/2e} path. This is likely due to incorrect positioning of the hydride with respect to the NH proton. To speed up the release of H_2 from the azadithiolate complexes along the {2H$^+$/2e} path, it would be important to favour a rotated geometry by substitution of two CO ligands at a single iron centre by a chelating donor ligand. This might also be critical to avoid a futile reduction loop that goes back to the starting material at an early stage of the reduction process. The reduction of a [$Fe_2(CO)_4$(κ^2-LL){μ-$SCH_2N(R)CH_2S$}] complex in the presence of acid may give access (possibly by concerted proton and electron transfer) to a terminal hydride ligand and restore a protonation site at the bridgehead N atom. However, the increased electron density at the diiron core that would inevitably result from the substitution of donor ligands for CO might also facilitate Fe–S bond cleavage upon reduction. The search for a compromise thus appears to be a key objective for improving the efficiency of azadithiolate complexes as electrocatalysts for proton reduction.

Experimental Section

Methods and materials: All experiments were carried out under an inert atmosphere by using Schlenk techniques for the syntheses. Acetonitrile (Merck, HPLC grade), *p*-toluenesulfonic acid monohydrate (Janssen), trifluoroacetic acid (Aldrich) and fluoroboric acid (diethyl ether complex, Aldrich) were used as received. The diiron complex [$Fe_2(CO)_6${μ-$SCH_2N(CH_2CH_2OMe)CH_2S$}] (**1**) and its *i*Pr analogue were prepared according to reported methods.[29]

The preparation and purification of the supporting electrolyte NBu_4PF_6 and the electrochemical equipment were as described previously.[29] All the potentials are quoted against the ferrocene/ferrocenium couple; ferrocene was added as an internal standard at the end of the experiments. ^{1}H NMR spectra were recorded on a Bruker AC300 spectrophotometer. The infrared spectra were recorded on a Nicolet Nexus Fourier transform spectrometer.

Protonation of 1: An orange solution of **1** (0.030 g, 0.0675 mmol) in CH_3CN (5 mL) turned yellow upon acidification with an excess of HBF_4/

Et_2O. The solution was evaporated to dryness and the residue washed with diethyl ether. Only the unprotonated complex **1** was recovered, as confirmed by FTIR and ^1H NMR spectroscopy. Protonation of **1** occurred in solution, as demonstrated by the FTIR solution spectrum (IR (CH_3CN): **1**: $\tilde{\nu}=2073$, 2034, 1996 (ν(CO)) cm^{-1}; **1-H$^+$**: $\tilde{\nu}=2089$, 2052, 2015, 1992 (ν(CO)) cm^{-1}), but it was not possible to isolate the protonated compound.

Digital simulations: All the simulations were performed with DigiElch Special Build Version 3 (Build SB3.600).[56] Details of the procedure are given as Supporting Information.

Acknowledgement

CNRS ("Programme Energie - PRI 4.1"), ANR (Programme "Photo-BioH2"), and Université de Bretagne Occidentale are acknowledged for financial support, and the Ministère de l'Education Nationale, de l'Enseignement Supérieur et de la Recherche for providing a studentship to S.E. Prs. C. J. Pickett and S. P. Best are gratefully acknowledged for helpful discussions.

[1] a) J. W. Peters, W. N. Lanzilotta, B. J. Lemon, L. C. Seefeldt, *Science* **1998**, *282*, 1853–1858; b) B. J. Lemon, J. W. Peters, *Biochemistry* **1999**, *38*, 12969–12973.

[2] a) Y. Nicolet, C. Piras, P. Legrand, C. E. Hatchikian, J. C. Fontecilla-Camps, *Structure* **1999**, *7*, 13–23; b) Y. Nicolet, A. L. de Lacey, X. Vernede, V. M. Fernandez, C. E. Hatchikian, J. C. Fontecilla-Camps, *J. Am. Chem. Soc.* **2001**, *123*, 1596–1602.

[3] For recent reviews, see : a) I. P. Georgakaki, L. M. Thomson, E. J. Lyon, M. B. Hall, M. Y. Darensbourg, *Coord. Chem. Rev.* **2003**, *238–239*, 255–266; b) M. Y. Darensbourg, E. J. Lyon, X. Zhao, I. P. Georgakaki, *Proc. Natl. Acad. Sci. USA* **2003**, *100*, 3683–3688; c) D. J. Evans, C. J. Pickett, *Chem. Soc. Rev.* **2003**, *32*, 268–275; d) T. B. Rauchfuss, *Inorg. Chem.* **2004**, *43*, 14–26; e) L.-C. Song, *Acc. Chem. Res.* **2005**, *38*, 21–28; f) V. Artero, M. Fontecave, *Coord. Chem. Rev.* **2005**, *249*, 1518–1535; g) S. P. Best, *Coord. Chem. Rev.* **2005**, *249*, 1536–1554; h) M. Bruschi, G. Zampella, P. Fantucci, L. De Gioia, *Coord. Chem. Rev.* **2005**, *249*, 1620–1640; i) X. Liu, S. K. Ibrahim, C. Tard, C. J. Pickett, *Coord. Chem. Rev.* **2005**, *249*, 1641–1652; j) L. Sun, B. Akermark, S. Ott, *Coord. Chem. Rev.* **2005**, *249*, 1653–1663; k) J.-F. Capon, F. Gloaguen, P. Schollhammer, J. Talarmin, *Coord. Chem. Rev.* **2005**, *249*, 1664–1676, and references therein.

[4] A list of recent (2005–2007) publications relating to different aspects of the chemistry of diiron models of $[FeFe]H_2$ases is provided as Supporting Information.

[5] a) F. Gloaguen, J. D. Lawrence, T. B. Rauchfuss, *J. Am. Chem. Soc.* **2001**, *123*, 9476–9477; b) F. Gloaguen, J. D. Lawrence, T. B. Rauchfuss, M. Bénard, M.-M. Rohmer, *Inorg. Chem.* **2002**, *41*, 6573–6582.

[6] a) X. Zhao, I. P. Georgakaki, M. L. Miller, J. C. Yarbrough, M. Y. Darensbourg, *J. Am. Chem. Soc.* **2001**, *123*, 9710–9711; b) X. Zhao, I. P. Georgakaki, M. L. Miller, R. Mejia-Rodriguez, C.-H. Chiang, M. Y. Darensbourg, *Inorg. Chem.* **2002**, *41*, 3917–3928.

[7] a) J.-F. Capon, S. El Hassnaoui, F. Gloaguen, P. Schollhammer, J. Talarmin, *Organometallics* **2005**, *24*, 2020–2022; b) D. Morvan, J.-F. Capon, F. Gloaguen, A. Le Goff, M. Marchivie, F. Michaud, P. Schollhammer, J. Talarmin, J.-J. Yaouanc, R. Pichon, N. Kervarec, *Organometallics* **2007**, *26*, 2042–2052; c) F. Gloaguen, D. Morvan, J.-F. Capon, P. Schollhammer, J. Talarmin, *J. Electroanal. Chem.* **2007**, *603*, 15–20; d) S. Ezzaher, J.-F. Capon, F. Gloaguen, F. Y. Pétillon, P. Schollhammer, J. Talarmin, R. Pichon, N. Kervarec, *Inorg. Chem.*, **2007**, *46*, 3426–3428.

[8] a) W. Dong, M. Wang, X. Liu, G. Li, F. Wang, L. Sun, *Chem. Commun.* **2006**, 305–307; b) W. Dong, M. Wang, T. Liu, X. Liu, K. Jin, L. Sun, *J. Inorg. Biochem.* **2007**, *101*, 506–513; c) S. Jiang, J. Liu, Z. Wang, B. Åkermark, L. Sun, *Polyhedron* **2007**, *26*, 1499–1504.

[9] a) G. Hogarth, I. Richards, *Inorg. Chem. Commun.* **2007**, *10*, 66–70; b) F. I. Adam, G. Hogarth, I. Richards, *J. Organomet. Chem.* **2007**, *692*, 3957–3968.

[10] J. L. Nehring, D. M. Heinekey, *Inorg. Chem.* **2003**, *42*, 4288–4292.

[11] K. Fauvel, R. Mathieu, R. Poilblanc, *Inorg. Chem.* **1976**, *15*, 976–978.

[12] R. Mejia-Rodriguez, D. Chong, J. H. Reibenspies, M. P. Soriaga, M. Y. Darensbourg, *J. Am. Chem. Soc.* **2004**, *126*, 12004–12014.

[13] a) J. D. Lawrence, H. Li, T. B. Rauchfuss, M. Bénard, M.-M. Rohmer, *Angew. Chem. Int. Ed.* **2001**, *40*, 1768–1771; b) H. Li, T. B. Rauchfuss, *J. Am. Chem. Soc.* **2002**, *124*, 726–727.

[14] a) S. Ott, M. Kritikos, B. Åkermark, L. Sun, R. Lomoth, *Angew. Chem. Int. Ed.* **2004**, *43*, 1006–1009; b) F. Wang, M. Wang, X. Liu, K. Jin, W. Dong, G. Li, B. Åkermark, L. Sun, *Chem. Commun.* **2005**, 3221–3223; c) S. Jiang, J. Liu, L. Sun, *Inorg. Chem. Commun.* **2006**, *9*, 290–292; d) W. Gao, J. Liu, B. Åkermark, L. Sun, *Inorg. Chem.* **2006**, *45*, 9169–9171; e) W. Gao, J. Liu, C. Ma, L. Weng, K. Jin, C. Chen, B. Åkermark, L. Sun, *Inorg. Chim. Acta* **2006**, *359*, 1071–1080; f) S. Jiang, J. Liu, Y. Shi, Z. Wang, B. Åkermark, L. Sun, *Dalton Trans.* **2007**, 896–902; g) W. Gao, J. Ekström, J. Liu, C. Chen, L. Eriksson, L. Weng, B. Åkermark, L. Sun, *Inorg. Chem.* **2007**, *46*, 1981–1991.

[15] a) L.-C. Song, J.-H. Ge, X.-F. Liu, L.-Q. Zhao, Q.-M. Hu, *J. Organomet. Chem.* **2006**, *691*, 5701–5709; b) L.-C. Song, J.-H. Ge, X.-G. Zhang, Y. Liu, Q.-M. Hu, *Eur. J. Inorg. Chem.* **2006**, 3204–3210.

[16] a) A. L. De Lacey, V. M. Fernandez, M. Rousset, R. Cammack, *Chem. Rev.* **2007**, *107*, 4304–4330; b) W. Lubitz, E. Reijerse, M. van Gastel, *Chem. Rev.* **2007**, *107*, 4331–4365, and references therein.

[17] a) Y. Nicolet, A. L. de Lacey, X. Vernede, V. M. Fernandez, C. E. Hatchikian, J. C. Fontecilla-Camps, *J. Am. Chem. Soc.* **2001**, *123*, 1596–1602; b) Y. Nicolet, B. J. Lemon, J. C. Fontecilla-Camps, J. W. Peters, *Trends Biochem. Sci.* **2000**, *25*, 138–143; c) Y. Nicolet, C. Cavazza, J. C. Fontecilla-Camps, *J. Inorg. Biochem.* **2002**, *91*, 1–8.

[18] a) R. H. Crabtree, J. A. Loch, K. Gruet, D.-H. Lee, C. Borgmann, *J. Organomet. Chem.* **2000**, *600*, 7–11; b) R. H. Crabtree, P. E. M. Siegbahn, O. Eisenstein, A. L. Rheingold, T. F. Koetzle, *Acc. Chem. Res.* **1996**, *29*, 348–354; c) E. Peris, J. C. Lee, Jr., J. R. Rambo, O. Eisenstein, R. H. Crabtree, *J. Am. Chem. Soc.* **1995**, *117*, 3485–3491; d) J. C. Lee, E. Peris, A. L. Rheingold, R. H. Crabtree, *J. Am. Chem. Soc.* **1994**, *116*, 11014–11019.

[19] A. J. Lough, S. Park, R. Ramachandran, R. H. Morris, *J. Am. Chem. Soc.* **1994**, *116*, 8356–8357.

[20] H. S. Shu, C. P. Lau, K. Y. Wong, W. T. Wong, *Organometallics* **1998**, *17*, 2768–2777.

[21] J. A. Ayllon, S. F. Sayers, S. Sabo-Etienne, B. Donnadieu, B. Chaudret, E. Clot, *Organometallics* **1999**, *18*, 3981–3990, and references therein.

[22] F. A. Jalon, B. R. Manzano, A. Caballero, M. C. Carrion, L. Santos, G. Espino, M. Moreno, *J. Am. Chem. Soc.* **2005**, *127*, 15364–15365.

[23] a) C. J. Curtis, A. Miedaner, R. Ciancanelli, W. W. Ellis, B. C. Noll, M. Rakowski DuBois, D. L. Dubois, *Inorg. Chem.* **2003**, *42*, 216–227; b) R. M. Henry, R. K. Shoemaker, R. H. Newell, G. M. Jacobsen, D. L. DuBois, M. Rakowski DuBois, *Organometallics* **2005**, *24*, 2481–2491; c) A. D. Wilson, R. H. Newell, M. J. McNevin, J. T. Muckerman, M. Rakowski DuBois, D. L. Dubois, *J. Am. Chem. Soc.* **2006**, *128*, 358–366; d) R. M. Henry, R. K. Shoemaker, D. L. DuBois, M. Rakowski DuBois, *J. Am. Chem. Soc.* **2006**, *128*, 3002–3010; e) A. D. Wilson, R. Shoemaker, A. Miedaner, M. Rakowski DuBois, D. L. Dubois, *Proc. Natl. Acad. Sci. USA* **2007**, *104*, 6951–6956; f) K. Fraze, A. D. Wilson, A. M. Appel, M. Rakowski DuBois, D. L. Dubois, *Organometallics* **2007**, *26*, 3918–3924, and references therein.

[24] a) L. Schwartz, G. Eilers, L. Eriksson, A. Gogoll, R. Lomoth, S. Ott, *Chem. Commun.* **2006**, 520–522; b) G. Eilers, L. Schwartz, M. Stein, G. Zampella, L. De Gioia, S. Ott, R. Lomoth, *Chem. Eur. J.* **2007**, *13*, 7075–7084.

[25] F. Wang, M. Wang, X. Liu, K. Jin, W. Dong, L. Sun, *Dalton Trans.* **2007**, 3812–3819.

[26] a) U. Koelle, S. Ohst, *Inorg. Chem.* **1986**, *25*, 2689–2694; b) U. Koelle, *New J. Chem.* **1992**, *16*, 157–169.
[27] I. Bhugun, D. Lexa, J.-M. Savéant, *J. Am. Chem. Soc.* **1996**, *118*, 3982–3983.
[28] D. A. Valyaev, M. G. Peterleitner, O. V. Semeikin, K. I. Utegenov, N. A. Ustynyuk, A. Sournia-Saquet, N. Lugan, G. Lavigne, *J. Organomet. Chem.* **2007**, *692*, 3207–3211.
[29] J.-F. Capon, S. Ezzaher, F. Gloaguen, F. Y. Pétillon, P. Schollhammer, J. Talarmin, T. Davin, J. E. McGrady, K. W. Muir, *New J. Chem.* **2007**, *31*, 2052–2064.
[30] S. J. Borg, T. Behrsing, S. P. Best, M. Razavet, X. Liu, C. J. Pickett, *J. Am. Chem. Soc.* **2004**, *126*, 16988–16999.
[31] S. J. Borg, J. W. Tye, M. B. Hall, S. P. Best, *Inorg. Chem.* **2007**, *46*, 384–394.
[32] a) M. H. Cheah, S. J. Borg, M. I. Blondin, S. P. Best, *Inorg. Chem.* **2004**, *43*, 5635–5644; b) M. H. Cheah, S. J. Borg, S. P. Best, *Inorg. Chem.* **2007**, *46*, 1741–1750.
[33] J. Windhager, M. Rudolph, S. Bräutigam, H. Görls, W. Weigand, *Eur. J. Inorg. Chem.* **2007**, 2748–2760.
[34] L.-C. Song, Z.-Y. Yang, Y.-J. Hua, U.-T. Wang, Y. Liu, Q.-M. Hu, *Organometallics* **2007**, *26*, 2106–2110.
[35] In contrast to its diiron analogue, the diruthenium hexacarbonyl complex with a μ-pdt bridge can be protonated at the metal–metal bond by HOTf in CH_2Cl_2: A. K. Justice, R. C. Linck, T. B. Rauchfuss, *Inorg. Chem.* **2006**, *45*, 2406–2412.
[36] C. Greco, G. Zampella, L. Bertini, M. Bruschi, P. Fantucci, L. De Gioia, *Inorg. Chem.* **2007**, *46*, 108–116.
[37] D. Chong, I. P. Georgakaki, R. Mejia-Rodriguez, J. Sanabria-Chinchilla, M. P. Soriaga, M. Y. Darensbourg, *Dalton Trans.* **2003**, 4158–4163.
[38] The analogue with R = *i*Pr has also been investigated under the same conditions as **1** (see Figure S1 in the Supporting InformationFc). As the nature of the R substituent has only a small effect on the redox potentials but does not affect the nature of the mechanisms, the results concerning $[Fe_2(CO)_6\{\mu\text{-}SCH_2N(iPr)CH_2S\}]$ are not detailed herein.
[39] a) The pK_a of HBF_4/Et_2O in MeCN is assumed to be the same as that of protonated diethyl ether,[40] that is, pK_a = 0.1.[41] However, for the simulations, we took an approximate value of 3 for pK_a(HBF_4/Et_2O), because in a solvent that is not rigorously anhydrous, protonation of residual water is expected to occur: the pK_a of H_3O^+ in MeCN is 2.3 ± 0.1;[42,43] b) For HOTs, we used pK_a = 8.3, as an average of the reported values.[44,45]
[40] X. L. Hu, B. S. Brunschwig, J. C. Peters, *J. Am. Chem. Soc.* **2007**, *129*, 8988–8998.
[41] K. Izutzu, *Acid-Base Dissociation Constants in Dipolar Aprotic Solvents*, IUPAC Chemical Data Series No. 35, Blackwell Scientific Publications, Oxford, **1990**.
[42] a) M. K. Chantooni, Jr., I. M. Kolthoff, *J. Am. Chem. Soc.* **1970**, *92*, 2236–2239; b) I. M. Kolthoff, M. K. Chantooni, Jr., *J. Am. Chem. Soc.* **1968**, *90*, 3320–3326; c) I. M. Kolthoff, S. Ikeda, *J. Phys. Chem.* **1961**, *65*, 1020–1026.
[43] J. F. Coetzee, D. K. McGuire, *J. Phys. Chem.* **1963**, *67*, 1810–1814.
[44] pK_a(HOTs) = 8.0 in MeCN: T. Fujinaga, I. Sakamoto, *J. Electroanal. Chem.* **1977**, *85*, 185–201.
[45] pK_a(HOTs) = 8.6 in MeCN: I. Leito, I. Kaljurand, I. A. Koppel, L. M. Yagupolskii, V. M. Vlasov, *J. Org. Chem.* **1998**, *63*, 7868–7874.
[46] The parameters i_p and E_p are respectively the peak current and the peak potential of a redox process; $E_{1/2} = (E_p^a + E_p^c)/2$, where E_p^a, i_p^a and E_p^c, i_p^c are respectively the potential and the current of the anodic and cathodic peaks of a reversible process; $\Delta E_p = E_p^a - E_p^c$. v [V s^{-1}] is the scan rate in CV experiments. An EC process comprises an electron-transfer step (E) followed by a chemical reaction (C).
[47] The potential of the peak around −1.4 V shifts negatively upon addition of acid.
[48] P. Das, J.-F. Capon, F. Gloaguen, F. Y. Pétillon, P. Schollhammer, J. Talarmin, *Inorg. Chem.* **2004**, *43*, 8203–8205.
[49] a) A. J. Bard, L. R. Faulkner, *Electrochemical Methods. Fundamentals and Applications*, Wiley, New York, **1980**, Chap. 11, pp. 429–485; b) E. R. Brown, R. F. Large in *Techniques of Chemistry, Vol. I, Physical Methods of Chemistry*, Part IIA, (Ed.: A. Weissberger), Wiley, New York, **1971**, Chap. 6, pp. 423–530.
[50] J.-M. Savéant, *Elements of Molecular and Biomolecular Electrochemistry—An Electrochemical Approach to Electron Transfer Chemistry*, Wiley, New York, **2006**, Chap. 2, pp. 78–181.
[51] X. Zhao, Y.-M. Hsiao, J. H. Reibenspies, M. Y. Darensbourg, *Inorg. Chem.* **2002**, *41*, 699–708.
[52] T. Liu, M. Wang, Z. Shi, H. Cui, W. Dong, J. Chen, B. Åkermark, L. Sun, *Chem. Eur. J.* **2004**, *10*, 4474–4479.
[53] G. Si, L.-Z. Wu, W.-G. Wang, J. Ding, X.-F. Shan, Y.-P. Zhao, C.-H. Tung, M. Xu, *Tetrahedron Lett.* **2007**, *48*, 4775–4779.
[54] a) C. Tard, PhD. Thesis, University of East Anglia, **2005**; b) C. J. Pickett, personal communication.
[55] D. T. Pierce, W. E. Geiger, *J. Am. Chem. Soc.* **1992**, *114*, 6063–6073, and references therein.
[56] For detailed information concerning DigiElch, see http://www.elchsoft.com and: a) M. Rudolph, *J. Electroanal. Chem.* **2003**, *543*, 23–29; b) M. Rudolph, *J. Electroanal. Chem.* **2004**, *571*, 289–307; c) M. Rudolph, *J. Comput. Chem.* **2005**, *26*, 619–632; d) M. Rudolph, *J. Comput. Chem.* **2005**, *26*, 633–641; e) M. Rudolph, *J. Comput. Chem.* **2005**, *26*, 1193–1204.
[57] EH calculations were performed with the CACAO package developped by Mealli and Proserpio: C. Mealli, D. M. Proserpio, *J. Chem. Educ.* **1990**, *67*, 399–402.
[58] Note that the peak at −1.4 V is not observed in the CV of **1** in the presence of acid until $[HBF_4]/[\mathbf{1}] > 3$ (Figure 1).
[59] Loss of H_2 from **1-3H$^+$** regenerates **1-H$^+$** and thus contributes to the reduction current at −1.2 V. It is therefore difficult to distinguish this reaction from the loss of H_2 from **1-2H**.
[60] The less negative catalytic proton reduction process (process I) reported by Pickett et al.[30] for $[Fe_2(CO)_6(\mu\text{-pdt})]$ was observed around −1.6 V versus Fc, which is 0.1 V less negative than the reduction potential of this complex in THF. Since the reduction of $[Fe_2(CO)_6(\mu\text{-pdt})]$ occurs at $E_{1/2} = -1.60$ V versus Fc in MeCN/NBu_4PF_6,[29] process I is expected to occur around −1.5 V in this electrolyte, which is similar to the acid-dependent reduction observed when CF_3CO_2H is added to a solution of **1** in MeCN, and only 0.3 V more negative than process A (−1.2 V, HA = HOTs or HBF_4; Scheme 5).
[61] J. W. Tye, M. Y. Darensbourg, M. B. Hall, *Inorg. Chem.* **2006**, *45*, 1552–1559.
[62] A. K. Justice, G. Zampella, L. De Gioia, T. B. Rauchfuss, J. I. van der Vlugt, S. R. Wilson, *Inorg. Chem.* **2007**, *46*, 1655–1664.
[63] S. Ezzaher, J.-F. Capon, F. Gloaguen, F. Y. Pétillon, P. Schollhammer, J. Talarmin, *Inorg. Chem.* **2007**, *46*, 9863–9872.
[64] This is the reverse of proton migration from the metal center to the N atom of the PNP ligand observed upon oxidation of $[HFe(PNP)(dmpm)(CH_3CN)]^+$ (PNP = $Et_2PCH_2N(Me)CH_2PEt_2$, dmpm = $Me_2PCH_2PMe_2$).[23d] A similar follow-up proton migration occurred upon oxidation of $[HNi(PNP)_2]^+$ to $[Ni(PNHP)(PNP)]^{2+}$, via Ni^{III} hydride complex $[HNi(PNP)_2]^{2+}$.[23a] This arises from the lowering of the pK_a of the Ni–H entity by more than 14 units upon one-electron oxidation of the metal.[23a] On the same grounds, metal-based reduction of the diiron complex in Scheme 9 is expected to result in an increased basicity of the metal site, which should be favourable to proton migration from the N atom to the iron centre.

Received: September 13, 2007
Revised: October 29, 2007
Published online: December 7, 2007

